

Review

# A Review of Research on Cavity Growth in the Context of Underground Coal Gasification

Huijun Fang<sup>1,2</sup>, Yuewu Liu<sup>3,4,\*</sup>, Tengze Ge<sup>1,2</sup>, Taiyi Zheng<sup>3,\*</sup>, Yueyu Yu<sup>1,2</sup>, Danlu Liu<sup>1,2</sup>, Jiuge Ding<sup>3</sup> and Longlong Li<sup>3</sup>

<sup>1</sup> China United Coalbed Methane National Engineering Research Center Co., Ltd., Beijing 100095, China

<sup>2</sup> PetroChina Coalbed Methane Company Limited, Beijing 100028, China

<sup>3</sup> Institute of Mechanics, Chinese Academy of Sciences, Beijing 100190, China

<sup>4</sup> School of Engineering Sciences, University of Chinese Academy of Sciences, Beijing 100049, China

\* Correspondence: author: lywu@imech.ac.cn (Y.L.); zhengtaiyi@imech.ac.cn (T.Z.)

**Abstract:** Underground Coal Gasification (UCG) is a leading-edge technology for clean and effective utilization of coal resources, especially for deep coal seams with a depth of more than 1000 m. Since the core operation place of UCG is the cavity, mastering the cavity growth pattern is a prerequisite to ensure the efficient and economic development of UCG. At present, scholars have conducted numerous research works on cavity growth, but the simulation conditions limit the research results. Hence, it is necessary to summarize and sort out the research results of cavity growth patterns, which contribute to deepening the understanding of UCG and pointing out the direction for subsequent research. First of all, this paper summarizes the development history of UCG technology and describes the cavity growth mechanism from chemical reactions and thermo-mechanical failure. Then, the research methods of cavity growth are summarized from three aspects: a field test, laboratory experiment, and numerical simulation. The results show that the appearance of the cavity is teardrop-shaped, and its growth direction is obviously related to the gas injection method, including the injection direction and rate. Subsequently, the factors affecting the cavity growth process are expounded from the geological factors (permeability, moisture content, and coal rank) and operating factors (temperature, pressure, gasification agent's composition, and gasification agent's flow pattern). Finally, the existing problems and development trends in the cavity growth are discussed. The follow-up research direction should focus on clarifying the cavity growth mechanism of the controlled-retractable-injection-point (CRIP) method of UCG in the deep coal seam and ascertain the influence of the moisture content in the coal seam on cavity growth.

**Keywords:** underground coal gasification; cavity growth; field test; laboratory experiment; numerical simulation



**Citation:** Fang, H.; Liu, Y.; Ge, T.; Zheng, T.; Yu, Y.; Liu, D.; Ding, J.; Li, L. A Review of Research on Cavity Growth in the Context of Underground Coal Gasification. *Energies* **2022**, *15*, 9252. <https://doi.org/10.3390/en15239252>

Academic Editors: Marek Laciak, Ján Kačur and Milan Durdán

Received: 2 November 2022

Accepted: 28 November 2022

Published: 6 December 2022

**Publisher's Note:** MDPI stays neutral with regard to jurisdictional claims in published maps and institutional affiliations.



**Copyright:** © 2022 by the authors. Licensee MDPI, Basel, Switzerland. This article is an open access article distributed under the terms and conditions of the Creative Commons Attribution (CC BY) license (<https://creativecommons.org/licenses/by/4.0/>).

## 1. Introduction

Carbon peaking and carbon neutralization are significant strategic goals of China's energy development. Clean and efficient coal utilization will contribute to achieving the dual-carbon strategy [1]. Underground Coal Gasification (UCG) refers to the controlled combustion of underground coal in situ to generate combustible gases such as CH<sub>4</sub>, H<sub>2</sub>, and CO [2]. UCG has changed the development mode of coal resources from traditional physical mining to chemical utilization, reducing the negative impact on the environment caused by coal mining. UCG is a leading-edge technology for effectively utilizing coal resources, especially for deep coal seams with a depth of more than 1000 m [3].

UCG has the following three unique advantages [3–5]: (1) Huge gasification potential. China's onshore coal resources with a depth of 1000–3000 m are predicted to be 3.77 trillion tons, equivalent to 272–332 trillion cubic meters of natural gas resources according to the calculation of UCG-producing rate of 40%. (2) Non-overlapping development. UCG's main target is the coal resources at buried depths of more than 1000 m, avoiding the traditional

coal-mining position and not competing for coal with the coal power and coal chemical industries. (3) Environmental protection. UCG in deep coal seams can avoid environmental risks such as surface collapse and shallow groundwater pollution. Moreover, the cavity after gasification can also be used to build natural gas or CO<sub>2</sub> storage.

The cavity is the core reaction site for UCG. Mastering the cavity growth pattern is a prerequisite to ensure the efficient and economic development of UCG. The cavity growth rate refers to the moving speed of the gasification surface in a specific direction, vertical by default. According to the test results of several UCG field tests, the cavity growth rate is 0.35~1.2 m/day [6]. Since the UCG process is conducted underground, it has the characteristics of non-visualization and uncontrollable multi-factors. As a result, the existent cognition of cavity growth patterns is incomplete at present, which needs further research to provide scientific evidence for future UCG engineering designs. The methods of cavity growth are experimental research (field test and indoor experiment) and numerical simulation research. For the field test, its advantage is to directly obtain the change law of the cavity shape and growth direction and provide the process parameters for the regular UCG operation. In contrast, its disadvantage is the vast cost of establishing a complete technological process test. Moreover, it is not easy to effectively control the cavity growth process due to the underground reaction. For experiment, its advantages are the controllable experimental conditions and the intuitive measurability of results, which are helpful in analyzing some basic laws of cavity growth. However, the applicability of the experimental results in the field project faces many challenges due to the large deviation between the experimental and actual UCG conditions. For numerical simulation, it can simulate the UCG process under various working conditions for mining scheme design and comparative evaluation. The prediction ability of models will be greatly reduced when the mechanism is unclear, or the data are biased. So it must be compared with field tests or experiment data [7]. The relevant progress will be introduced in detail in Section 3.

In this paper, research contributions are reported according to the following sections. In Section 2, we review the development history of UCG technology and describe the cavity growth mechanism from chemical reactions and thermo-mechanical failure. In Section 3, we discuss the research methods of cavity growth which are summarized from three aspects: a field test, laboratory experiment, and numerical simulation. In Section 4, we analyze the influencing factors affecting the cavity growth from the geological factors and operating factors. In Section 5, we summarize the existing problems and discuss the development trends involved in cavity growth research.

## 2. Research Progress of UCG and Cavity Growth

### 2.1. UCG Development History

The history of UCG stretches back 150 years to 1868. During the process, it has achieved the transformation from concept to technology. The significant milestones mainly include:

In 1868, William Siemens of the United Kingdom first proposed to move a surface gasifier to an underground coal mine to directly gasify coal, marking the proposal of the UCG concept. In 1888, Dmitri Mendeleev of Russia expressed the basic technological process idea of UCG. In 1910, Anson Betts of the United States clarified the specific implementation of UCG based on three technology patents. In 1912, William Ramsay of UK completed the first industrial test of UCG [8]. In the following 100 years, UCG technology has successively formed shaft-type development and shaft-less development [3].

The shaft-type UCG technology consists of a borehole mode and long tunnel mode [9]. The borehole UCG mode is to drill rows of air intake and outlet holes into the coal seam according to a certain network layout on the surface. In the borehole UCG mode, the ignition position is at the intake hole, and the gas produced by gasification is expelled from the gas outlet hole via channel blast method. In the 1930s~1960s, the Soviet Union conducted a borehole field test for the first time, successfully realized coal gasification in a shallow coal seam, and achieved economic benefits. The long tunnel UCG mode is to establish a gasification tunnel in the coal seam by manual excavation, where the gasification

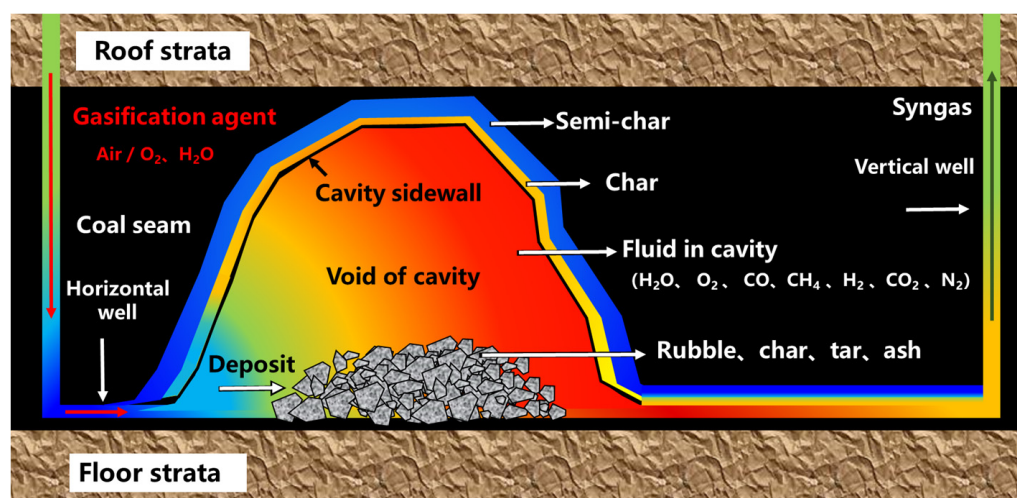
agent reacts with the coal in the tunnel via the channel blast method. The long tunnel UCG mode was developed from the borehole UCG mode in China based on the Soviet Union. In the 1950s~1980s, China mainly carried out long tunnel UCG mode field tests, forming a gasification technology with “long channel, large section and two stages”.

The shaft-less (drilling-type) UCG mode is to use drilling technology to build injection and production wells in the coal seam, and then establish a gasification channel between the two wells by linking methods including reverse combustion, electric resistive heating, hydraulic fracturing, and directional drilling [9,10]. As shown in Figure 1, the drilling-type UCG mode can be divided into the linked-vertical-wells (LVW) technique and controlled-retractable-injection-point (CRIP) technique according to the layout of gas injection wells. The LVW-type gas injection well is perpendicular to the coal seam, and the CRIP-type is parallel to the coal seam. The LVW technique was the earliest shaft-less UCG mode that the Soviet Union developed for decades. In the 1970s~1980s, the Lawrence Livermore National Laboratory of the United States developed a CRIP gasification process based on horizontal well-drilling technology. The CRIP technology can effectively control the gasification process, increase the utilization area of underground coal, and reduce the gasification cost. CRIP technology is a new milestone for UCG. Since then, it has been adopted by almost all field tests and has played a considerable role in the current UCG field test in the deep coal seam. In 2009~2011, the CRIP was used to conduct a UCG industrial field test in the deep coal seam in Swan Hills, Alberta, Canada. The target coal seam of this test was buried at a depth of about 1400 m, as was the deepest UCG test so far. Moreover, China completed CRIP UCG tests in Ulanqab of Inner Mongolia from 2007 to 2015.

Compared with the shaft-type UCG technology, the drilling-type UCG mode reduces the construction conditions of the gasification channel and increases the utilization depth of coal resources. It is the current mainstream development method for UCG. Therefore, this paper is organized around the drilling-type UCG mode.

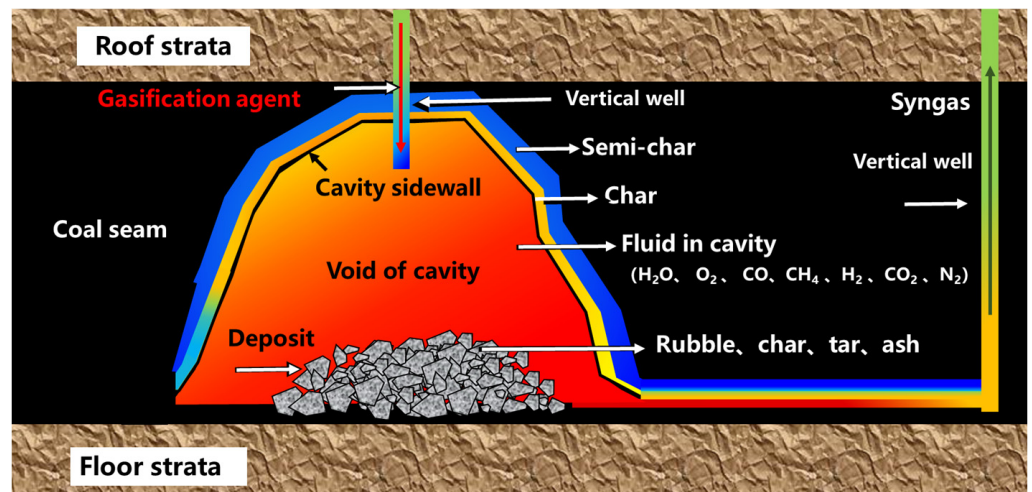
## 2.2. Cavity Growth Mechanism

From Figure 1, the cavity is the core reaction site for UCG, including the sidewall, void space, and deposit region [11,12]. The sidewall is the boundary that defines the cavity, which is divided into the roof strata boundary, the floor strata boundary, and the coal seam sidewall boundary. For the coal seam sidewall boundary, there are a char layer, semi-char coal, dry coal, and raw coal toward the interior of the coal seam. The void space is the cavern formed in coal seams after solid carbon is consumed. The deposit region is formed by the damage and collapse of the coal walls of the cavity, containing coal ash, coal lumps, char, crushed stone, tar, etc.



(a) LVW-type

Figure 1. Cont.



(b) CRIP-type

Figure 1. Schematic diagram of the drilling-type UCG mode (modified from [7]).

The cavity growth process occurs at the gas–solid interface, manifested in that the carbon on the side coal wall is constantly consumed or collapsed by combustion and gasification. The process is strongly related to the chemical reaction and thermo-mechanical failure on the side wall [13–15].

For the chemical reaction, Zou et al. [3] and Bhutto et al. [16] pointed out that the essence of UCG was the mutual thermochemical equilibrium process between the solid-phase carbon and the gas-phase  $O_2$ , water vapor,  $CO_2$ , and  $H_2$ . There were reaction zones suitable for an oxidation reaction, reduction reaction, and dry distillation reaction in sequence along the gasification channel axis. The difference in chemical reaction rates in various reaction zones directly determined the coal consumption rate on the side wall, which affected the cavity's geometry and expansion rate.

For the thermo-mechanical failure, as shown in Figure 2, Bhaskaran et al. [17] and Niu et al. [18] indicated that a large amount of heat released by coal combustion and gasification first evaporated the free moisture in the raw coal, leading to the expansion of surface pores and micro-cracks. Then, more microcracks were generated by thermal stress. With the further evaporation of the bound water in the raw coal, the coal skeleton structure would break and collapse, resulting in significant fractures. Subsequently, numerous intertwined fractures were produced by releasing volatile substances and liquid tar in the raw coal. Finally, under gravity, the coal rubble fell off from the total coal mass due to local thermal stress rupture or global thermal stress collapse.

In the actual UCG process, the effects of the chemical reaction and thermo-mechanical failure on the cavity growth are not independent but interactive and complementary.

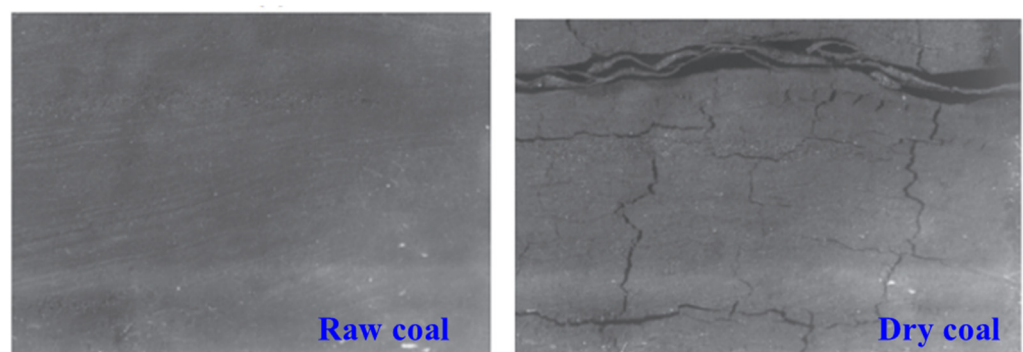
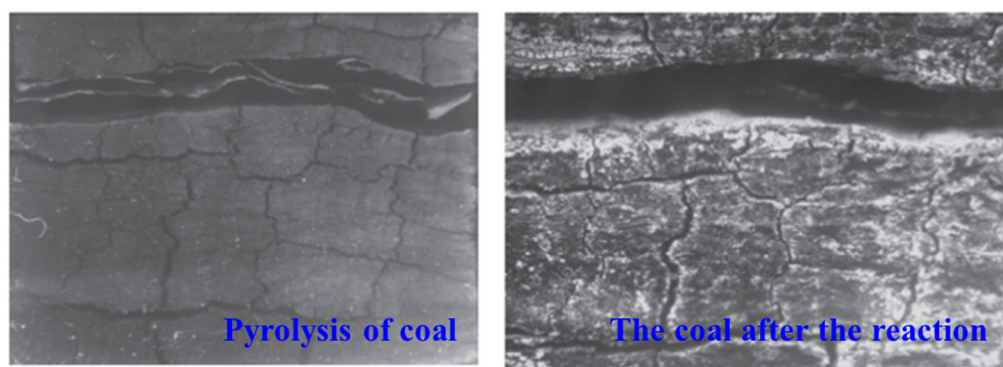


Figure 2. Cont.



**Figure 2.** Microscopic images of coal during continuous heating (edited from [17]).

### 3. Current Status of Research Methods for Cavity Growth

#### 3.1. Field Test

##### 3.1.1. Direct Observation Method

Currently, the field tests that can visually demonstrate the cavity growth process are basically located in the surface coal seams, and only a few field test results have been publicly reported.

In 1976~1979, the Hoe Creek coal mine in the United States successively conducted three phases of UCG tests with a buried depth of about 40 m. Of these, the most valuable tracer studies came from the Hoe Creek II trial. In this test, it was observed that the longitudinal growth rate of the cavity was faster than the horizontal growth rate, and the cavity was almost filled with a large amount of gravel [19].

In 1981~1982, the Centralia Coal Mine in the Tono Basin, Washington, USA successfully conducted large-scale UCG tests, codenamed LBK-1~LBK-5, in five blocks. Among them, LBK-1 used CRIP technology for the first time to complete the injection of gasification agent and the production of syngas. The uniqueness of the LBK-1 test is that the UCG process is completed in the coal seam outcrop on the surface, where the generated cavity could be excavated [9]. The cavity excavated after gasification is shown in Figure 3; the cavity profile was generally similar to oval, and the aspect ratio of the cavity profile was between 1.3:1 and 1.7:1. Moreover, the boundaries of the void area, rubble area, and ash area in the cavity were evident from top to bottom. The void area was located at the upper part of the cavity, in the shape of an inverted bowl. The rubble area was in the middle area, consisting of dry coal, char, and crushed stone. At the same time, the ash area was confined to the cavity bottom [20,21].

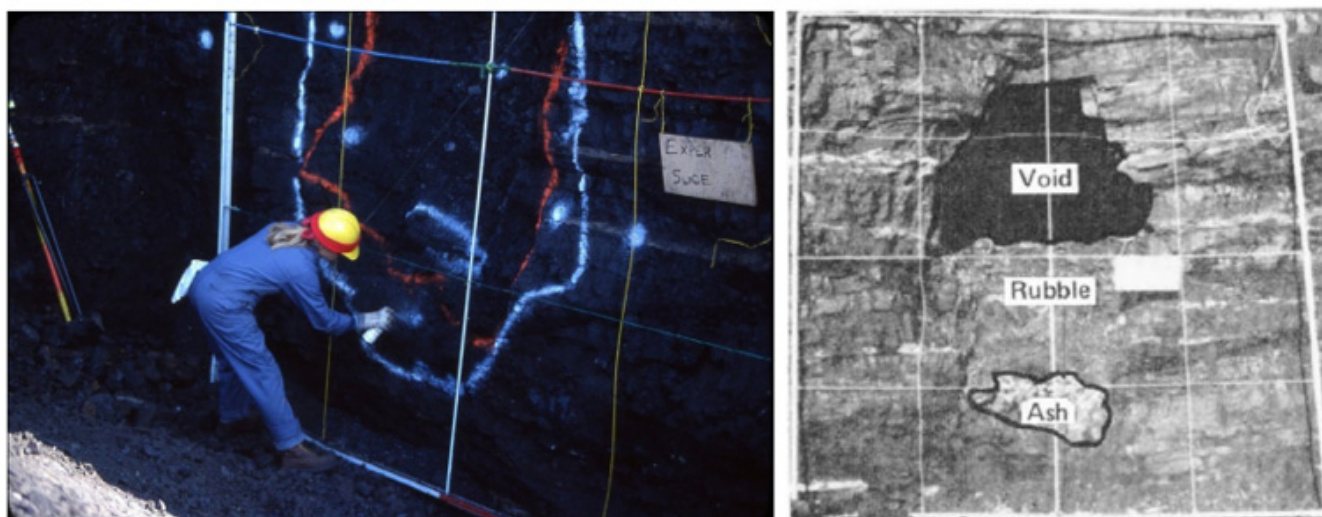
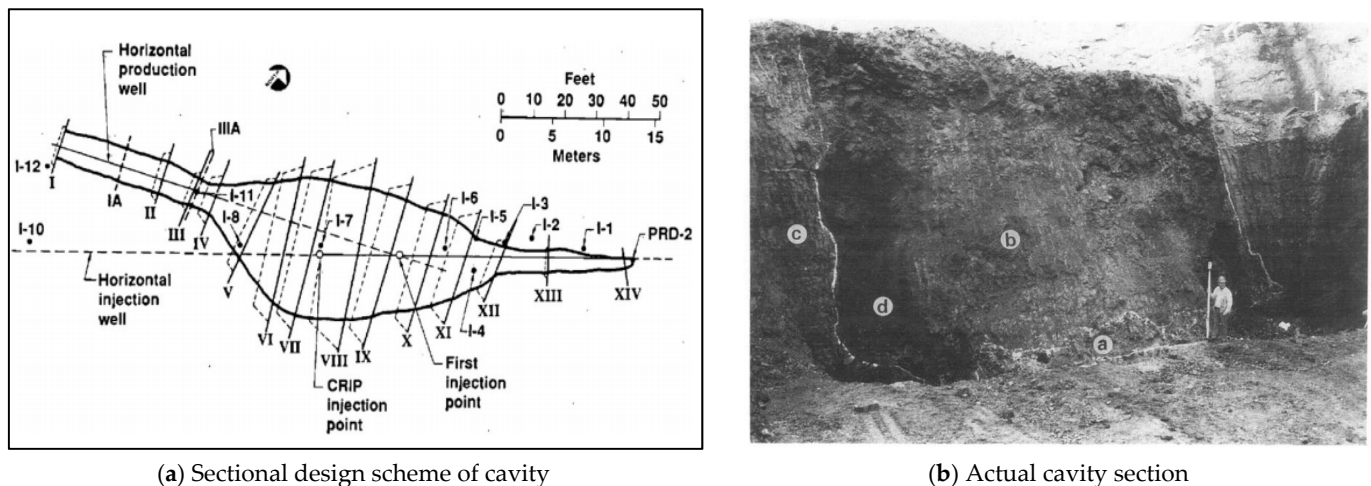


**Figure 3.** The cavity for large UCG trial at Centralia mine (from [21,22]).

In 1983, Centralia proceeded with another large-scale CRIP-UCG test, which lasted 30 days and consumed 2000 t of coal mass. As shown in Figure 4, the multi-position sliced excavation operation was adopted for the cavity in this trial. The results showed that the cavity growth direction was first extended to the coal seam roof and then laterally expanded along the roof. Along the path of the syngas outflow channel, the combustion residue area composed of the rubble area and the ash area gradually formed a V shape. Moreover, the closer to the production well, the more the proportion of dry coal and char in the combustion residue, while the lower the roof gravel and coal ash content, or it even did not exist [23–25].



(a) Sectional design scheme of cavity

(b) Actual cavity section

**Figure 4.** Cavity for large-scale CRIP-UCG trial at Centralia mine (from [23,26]).

### 3.1.2. Indirect Observation Method

Restricted by technical means and test costs, the cavity cannot be observed by direct excavation when the coal seam buried depth exceeds a specific limit. Thus, the cavity growth process can only be interpreted by the indirect method.

The cavity can be described by drilling the core of the post-combustion coal seam to obtain growth characteristics, such as the extent of the cavity area and the degree of roof collapse. In 1987–1988, the Rocky Mountain I UCG project, with a burial depth of 110 m, was tested in the United States. As indicated in Figure 5, the analysis of the drilled cores confirmed that the cavity width was about three times the thickness of the gasified coal when sufficient gasification time was allowed. In addition, the void space within the cavity was relatively small and unevenly distributed. In the area where the rock fell off, the gravel material accounted for about 25–50% of the cavity height [27,28].

The shape of the cavity can also be observed by using ground penetrating radar (GPR) technology. The UCG test in Barbara, Poland obtained a cavity profile with a monitoring accuracy of 5–10 cm by applying GPR technology, as illustrated in Figure 6 [29].

### 3.2. Laboratory Experiment

There are apparent discrepancies in the cavity growth behaviors corresponding to the LVW and CRIP types. To analyze the cavity growth process more precisely, researchers have accomplished a series of physical experiments at different scales.

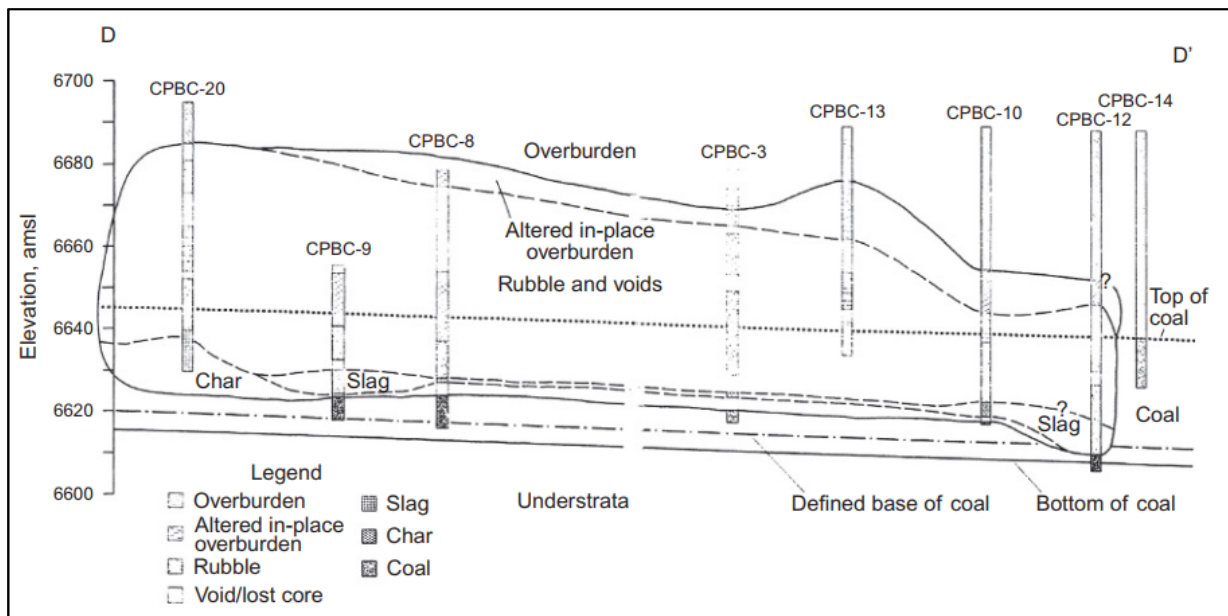


Figure 5. D-D section view of the cavity of the CRIP UCG test at Rocky Mountain I, USA (from [27]).

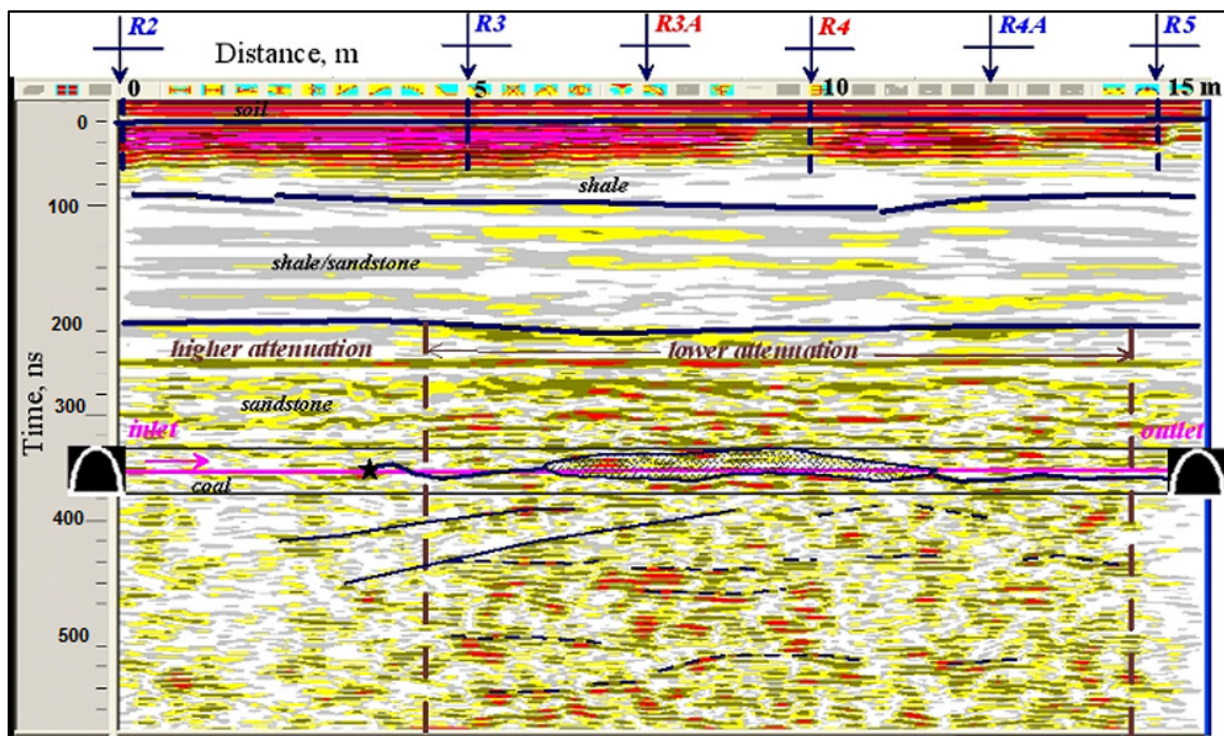


Figure 6. GPR monitoring section of the cavity of the UCG test in Barbara, Poland (from [29]).

### 3.2.1. Small Scale Experiments

Taking LVW technology as the research background, Daggupati et al. [30,31] conducted borehole combustion experiments on lignite with a size of  $(30\text{--}40) \times 20 \times 15$  cm. The experimental setup is displayed in Figure 7. The injection well and production well with a diameter of 3 mm were drilled from the coal block top surface to a position 4 cm above the coal block bottom. The two wells were connected by a 3mm-diameter horizontal well. Meanwhile, a temperature-monitoring channel with a diameter of 1 mm was drilled in the coal block. The surface of the coal blocks was covered with refractory bricks. The bricks were enclosed by cement to avoid gas and temperature leakage. The component of the



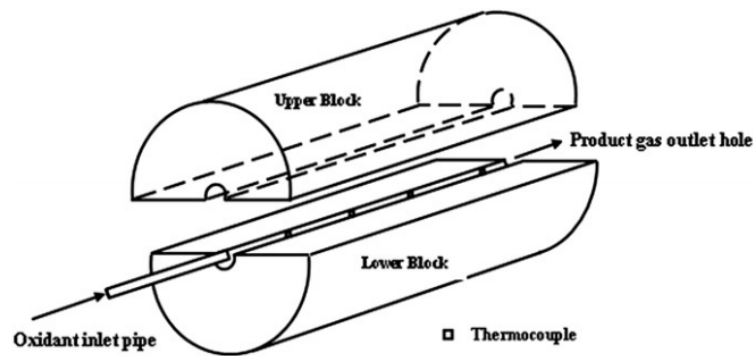
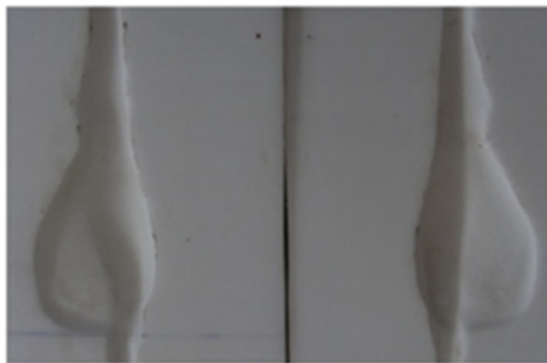


Figure 9. Experimental device for CRIP technology (from [32]).



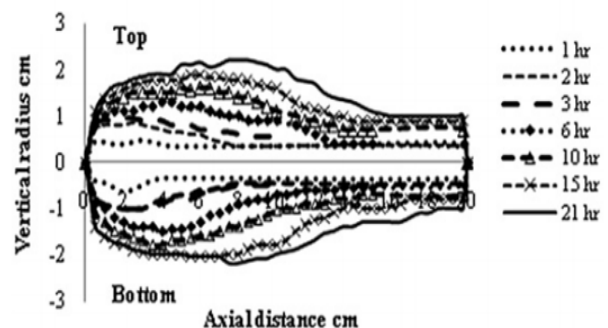
(a) camphor,  $11 \times 10 \times 24$  cm



(b) wood, length 35–62 cm, diameter 14–22 cm



(c) coal,  $8 \times 12 \times 24$  cm



(d) cavity profile over time

Figure 10. Cavity growth behavior of CRIP technology (from [32]).

### 3.2.2. Large Scale Experiments

In sequence, Kapusta et al. [33,34] conducted CRIP UCG tests on lignite coal of  $5.7 \times 0.8 \times 0.8$  m and  $2.6 \times 1.0 \times 1.1$  m with two large-scale experimental platforms under atmospheric pressure. In experiments, the change in coal temperature recorded by thermocouple was used to describe the cavity growth process. The experimental setup is shown in Figure 11. An important part of the unit was the gasification chamber, 7 m in length, which allowed oxygen, air and steam to be supplied individually or in combination as gasification agents. The experimental results are shown in Figure 12. The gasification chamber extended upward from the coal block bottom. Due to the low injection rate of the gasification agent, it could react uniformly with coal, resulting in a symmetrical round shape of the cavity. After expanding to the top surface, the cavity began to develop towards the flow direction of the gasification agent. In Figure 12c, the reason for the leftward shift of the cavity was that the collapsed roof partially blocked the gas injection channel.

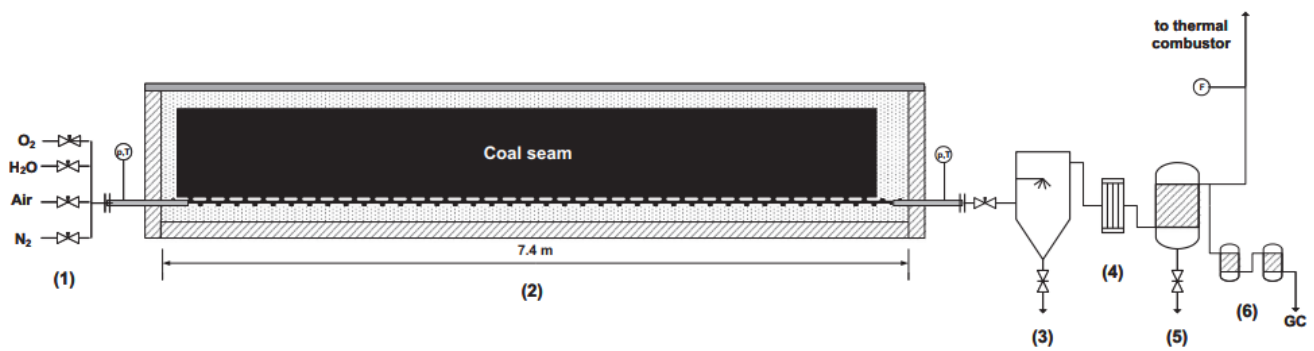


Figure 11. Schematic diagram of large-scale UCG experimental device (from [34]).

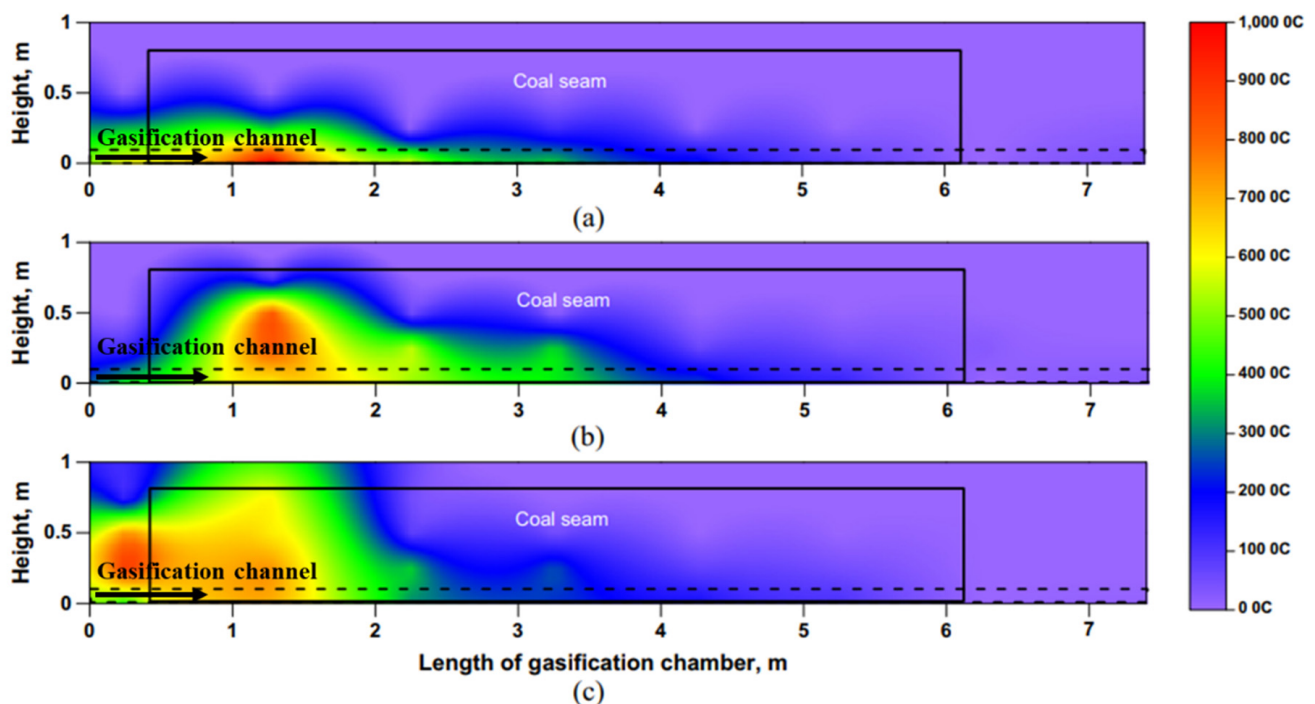


Figure 12. Temperature distribution in the UCG device (a) 20 h (b) 70 h (c) 110 h (from [34]).

Wang et al. [35] used an analogous experimental device to conduct UCG simulation experiments on China's Ulanqab lignite and observed the variation in the temperature field inside the coal during gasification.

### 3.3. Numerical Simulation

The field test requires a massive amount of material resources. Limited by equipment, it is difficult to observe the complete gasification process in laboratory experiments. Therefore, numerical simulation is needed to enhance the understanding of the gasification process.

In the numerical simulation, the actual cavity shape is simplified into regular geometric shapes, such as rectangular or teardrop shapes. Then, the numerical model of the cavity growth is established by combining the mathematical equations of mass transfer, heat transfer, and mechanics. Perkins [11] summarized the governing equations related to UCG, as shown in Table 1.

**Table 1.** Governing equations related to UCG [from [11]].

No.	Set	Equation
1	Conservation of mass	$\frac{\partial}{\partial t} (\varnothing_{\beta} \rho_{\beta}) + \nabla \cdot (\rho_{\beta} \vec{u}_{\beta}) = \dot{\omega}_{\beta}$
2	Conservation of species	$\frac{\partial}{\partial t} (\varnothing_{\beta} \rho_{\beta} Y_{\beta}^i) + \nabla \cdot (\rho_{\beta} \vec{u}_{\beta} Y_{\beta}^i) = \nabla \cdot (\rho_{\beta} D_{\beta}^i \nabla Y_{\beta}^i) + \dot{\omega}_{\beta}^i$
3	Conservation of momentum	$\frac{\partial}{\partial t} (\varnothing_{\beta} \rho_{\beta} \vec{u}_{\beta}) + \nabla \cdot (\rho_{\beta} \vec{u}_{\beta} \otimes \vec{u}_{\beta}) = -\nabla P - \nabla \cdot \tau_{\beta} + k \cdot k_r \vec{u}_{\beta} + \varnothing_{\beta} \rho_{\beta} \vec{g}$
4	Conservation of energy	$\sum_{\beta} \varnothing_{\beta} \rho_{\beta} U_{\beta} + (1 - \epsilon_r) \rho_r U_r + \sum_{\beta} \nabla \cdot (\varnothing_{\beta} \rho_{\beta} \vec{u}_{\beta} h_{\beta})$ $= \nabla \cdot (\lambda_{eff} \nabla T) + \sum_{\beta} \sum_i \nabla \cdot (h_{\beta}^i \rho_{\beta} D_{\beta}^i \nabla Y_{\beta}^i) + \dot{q}_{well}$
5	Conservation of turbulent kinetic energy	$\frac{\partial}{\partial t} (\varnothing_{\beta} \rho_{\beta} k) + \nabla \cdot (\rho_{\beta} \vec{u}_{\beta} k) = \nabla \cdot (\varnothing_{\beta} (\mu_{\beta} + \frac{\mu_t}{\sigma_k}) \nabla k) + \varnothing_{\beta} (G - \rho_{\beta} \epsilon) + S_{k2} + \dot{\omega}_k$
6	Conservation of energy dissipation	$\frac{\partial}{\partial t} (\varnothing_{\beta} \rho_{\beta} \epsilon) + \nabla \cdot (\rho_{\beta} \vec{u}_{\beta} \epsilon) = \nabla \cdot (\varnothing_{\beta} (\mu_{\beta} + \frac{\mu_t}{\sigma_k}) \nabla \epsilon) + \varnothing_{\beta} \frac{\epsilon}{k} (C_{1\epsilon} G - C_{2\epsilon} \rho_{\beta} \epsilon) + \dot{\omega}_{\epsilon}$
7	Conservation of species at wall	$-\sum_{j=1}^{N_g} \dot{\omega}_W^j Y_W^j - \frac{\rho_W}{\delta_n} D_{M,i} (Y_W^i - Y_g^i) + W_i \sum_{k=1}^{N_w} v_{i,k} r_{k,wall} = 0$
8	Stress tensor for each phase $\beta$	$\tau_{\beta} = -\varnothing_{\beta} \mu_{\beta} \left[ \nabla \vec{u}_{\beta} + \nabla \vec{u}_{\beta}^T \right] - \frac{2}{3} \nabla \cdot \vec{u}_{\beta} I$
9	Source term for phase $\beta$	$\dot{\omega}_{\beta} = \sum_{i=1}^{N_c} \dot{\omega}_{\beta}^i$
10	Source term for species $i$ phase $\beta$	$\dot{\omega}_{\beta}^i = \sum_{\alpha=1}^{N_p} \dot{\omega}_{\alpha,\beta}^i + \dot{\omega}_{well,\beta}^i + \dot{\omega}_{react,\beta}^i$
11	Interphase constraint	$\dot{\omega}_{\alpha,\alpha}^i = 0$
12	Reaction source for species $i$ phase $\beta$	$\dot{\omega}_{react,\beta}^i = W_{\beta}^i \sum_{k=1}^{N_R} v_{i,k} \dot{r}_k$
13	Mass transfer of matter	$\frac{\partial C_i}{\partial t} + \nabla \cdot (-D_i \nabla C_i) + \vec{u} \cdot \nabla C_i = \dot{\omega}_{react,\beta}^i$

### 3.3.1. One-Dimensional Numerical Model

In 1976, Winslow [36] established a one-dimensional time-dependent simulation model by combining mass conservation equations, energy conservation equations, reaction kinetics, and Darcy's law of seepage. The model simulated the gasification process of coal with a length of 30 cm under 0.48 MPa. The coal gasification process was regarded as the mass transfer process of gaseous and condensed species in porous media. Moreover, the model can obtain the temperature, substance concentration, and gas flow velocity distribution at different locations with time. The simulation results showed that the peak temperature was about 1200 K, and the moving speed of the gasification front was 5 cm/h. During the gasification process, the char zone was dominated by the reactions with steam and oxygen, the pyrolysis zone and the coal drying zone was formed, and the gas phase was mainly distributed in the char zone and the pyrolysis zone.

In 1980, Tsang [37] established a 1D coal gasification model considering multi-component gas diffusion. According to the reaction characteristics, the model divided the coal into three regions: carbonized coal, dry coal, and raw coal. The coal consumption process was reflected by observing the changes in the above regions.

In 1983, Massaquoi and Riggs [38,39] simulated the gasification process of wet coal for the first time. The model considered the evaporation of coal moisture, the movement of the evaporation front, transpiration cooling effect of the water vapor and pyrolysis gases, pyrolysis and char/gas reactions occurring in dry coal regions, Darcy flow of steam and gases through coal, changes in porosity and permeability of coal, temperature-dependent coal physical properties, multicomponent diffusion in ash and gas films, and oxidation reactions in ash. The model completed the calculation of the combustion location, combustion rate, and combustion temperature. Moreover, the model also analyzed the influence of ambient temperature, ash layer thickness, coal moisture content, and mass transfer coefficient on the gasification process.

In 1987, Park and Edgar [40], based on the Massaquoi and Riggs models, established a 1D unsteady numerical model including the coal ash region, dry coal region, and wet coal region. In addition to further considering the shrinkage of coal, the model introduced the Arrhenius chemical reaction rate expression into the coal pyrolysis reaction, so that the temperature and the reaction rate were related. Moreover, the model equated the coal consumption rate with the cavity growth rate. By comparing the experiment result, it was determined that the lateral cavity growth rate was 1~3 cm/h in the coal gasification periods.

Thereafter, Perkins and Sahajawalla [41–43] combined multi-component diffusion and natural convection processes, and further discussed the operating conditions (pressure, temperature, water inflow, and gas composition) and coal characteristics (thermal stress spalling behavior, reactivity, and composition) on the cavity growth rate and energy efficiency.

At this point, the basic UCG theoretical model of cavity growth for coal chemical reactions has been basically constructed.

The 1D numerical model can simulate the the gasification region's heat and mass transfer process via Darcy's seepage law, energy conservation equation, mass conservation equation, reaction kinetics, and other mathematical equations. However, the biggest limitation of the 1D numerical model is that it can only simulate the coal gasification process in a single direction. It is hard to comprehensively reflect the overall evolution of the cavity, such as the influence of the gasification agent flow path and coal collapse on the cavity growth.

### 3.3.2. Two-Dimensional Numerical Model

In 2009, Luo et al. [44] established a cavity growth numerical model for LVW technology based on the mathematical equations of the one-dimensional model and considering both natural convection and strong convection equations. This model fixed the cavity boundary at a specific time node. The model analyzed the cavity growth behavior by connecting the coal consumption at multiple sequential time nodes. The model predicted that the coal consumption in 25 days was 2436.6 tons under the background of the Hanna II UCG test in the United States, and in 38 days was 4139.3 tons under the background of the Hanna III UCG test. The error between field test results and simulation results was less than 5%.

In 2016~2018, Samdani et al. [45–47] predicted cavity growth based on models for LVW technology, where the cavity was divided into a rubble zone, void zone, and roof zone. The models considered reaction kinetics, heat transfer, mass transfer, and coal spalling effects. Specially, the model adopted non-ideal flow patterns in different zones, replacing the model of the unified flow field of previous scholars. The simulation predictions for the cavity growth rate and outlet gas mass matched well with laboratory observations.

The cavity growth process can be demonstrated by not only the mass variation of consumed coal, but also the change in the temperature field. In 2014, Xin et al. [48] simulated the temperature distribution field of the surrounding rock of the cavity under different boundary conditions by using the comsol software, and determined the range of the charred surrounding rock and the coking cycle process of coal wall.

The 2D numerical model inherits and develops the mathematical equations of the one-dimensional numerical model, which improves the theoretical basis for cavity evolution. Combined with the more complex geometric boundary conditions, the 2D numerical model can intuitively reflect the basic physical and chemical change process of UCG via the cloud images. At present, the 2D numerical model research focuses on the influence of gasification process parameters such as gasification agent ratio and flow rate on the cavity growth.

### 3.3.3. Three-Dimensional Numerical Model

Some 3D models are simulated based on the geometric boundary of the formed and fixed cavity. In 2010, Daggupati et al. [30] built a CFD numerical cavity model with a teardrop-shaped geometric appearance, where the physical fields only involved heat transfer and free flow fields. The advantage of this model was that the flow pattern in the

cavity could be analyzed by calculating the velocity at any point or section in the cavity and predicted the cavity growth direction combined with the temperature distribution. In 2018, Jowkar et al. [49] introduced a series of time-dependent boundary equations and combined them with Comsol software to build a teardrop-shaped cavity growth model.

Without fixed cavity boundaries, the cavity growth process can also be dynamically displayed through the variation in the coal concentration field. In 2010, Nourozieh et al. [50] established a 3D UCG model via the STARS module of CMG software, and studied the cavity growth process, temperature distribution, and syngas composition in a deep coal seam. In 2013, Shirazi et al. [51] established an isometric computational fluid dynamics (CFD) model ( $3 \times 1.5 \times 2$  cm) that can describe the cavity growth process based on the experimental data of small core gasification. The model clearly showed the changes in temperature field and concentration field during gasification, and analyzed the sensitivity of the effects of coal permeability, coal thermophysical properties, and gasification agent flow rate on the gasification process.

Different from the single gasification cavity model mentioned above, in 2011, Seifi et al. [52] applied the CMG software STAR module to further simulate the developing process from a single cavity to multiple cavities under the CRIP method. In 2017, Kasani et al. [53] used CMG software and FLAC3D software to build a numerical model of multi-cavity growth considering stress changes. The unique feature of this model was that it could not only describe the changes in the temperature field and concentration field of the cavity, but also reflect the change in the shear stress at the cavity boundary. Furthermore, by analyzing the concentration of shear stress, the model was capable of assisting in determining the location where the coal wall of the cavity was prone to fall off or the overlying rock cracks. In 2022, through CMG software, Jiang et al. [54] constructed a large-scale 3D UCG model with an improved CRIP method, which is more suitable to deep UCG.

The mathematical equations of the 3D model are consistent with the 2D model. The 3D model is constructed by linking a series of CFD sub-models, which is convenient for simulating the entire UCG process. The simulated contents of the 3D model and 2D model are basically the same, but the 3D model is closer to reality in the analysis of results. At present, the main problems facing 3D models focus on the poor coupling adaptability of physical–chemical field coupling and excessive computational load.

### 3.4. Chapter Summary

This section summarizes the current research methods of cavity growth from three aspects: field test, laboratory experiment, and numerical simulation.

Field test research can be classified into the direct observation method and indirect observation method. The direct observation method is to observe the cavity shape by excavating the coal seam outcrop after gasification. The indirect observation methods are the drilling core analysis method and the GPR technology analysis method. Although researchers originally gained a basic understanding of the cavity growth process from field tests, field test research is now rarely used due to the high cost of testing and the difficulty in performing sensitivity analyses of production factors.

Laboratory experimental research includes small-scale experiments and large-scale experiments. The laboratory experiment simplifies the production conditions of UCG based on the similarity criterion, which can characterize the cavity growth process in more detail and provide the basis of parameter selection for the numerical simulation study. In the experiment, the cavity growth pattern is analyzed through direct observation of the morphology of combustible materials after gasification or indirect temperature monitoring. The results show that the appearance of cavity is teardrop-shaped, and its growth direction is obviously related to the gas injection method. At present, the existing experimental equipment can only withstand the low-pressure environment, and it is difficult to simulate the high-pressure conditions of the UCG in the deep coal seam.

Numerical simulation is the main method to study cavity growth patterns. With the rise and development of computational simulation technology, the numerical simulation modeling method has developed from 1D model to 3D model. The mathematical equations have become more accurate in representing the cavity growth mechanism, and the simulation results are closer to reality.

#### 4. Influencing Factors of Cavity Growth

In the cavity growth process, the interaction of influencing factors makes the physical and chemical processes of UCG extremely complex. In general, the cavity growth process is mainly controlled by geological factors and operating factors [6,42].

##### 4.1. Geological factors

###### 4.1.1. Coal Seam Physical Properties

Coal seam physical properties mainly include permeability and moisture content.

The permeability of coal determines the flow path of the gasification agent and then affects the shape of cavity. Shirazi et al. [51] established three groups of LVW UCG models with the permeability of 1 mD, 100 mD, and 10 D, respectively, through CFD software. The results indicated that when the permeability of the coal seam was 1 mD, the cavity growth process was suppressed. The growth direction was mainly along the flow channel, showing that the cavity shape was relatively flat. When the permeability was 100 mD, the cavity growth was further expanded in the vertical direction, resulting in the cavity being teardrop-shaped. When the permeability was 10 mD, the flow resistance of the gasification agent in the coal seam was reduced, contributing to the cavity growth in the vertical and horizontal direction. On this occasion, the cavity shape was approximately hemispherical. Similarly, through numerical simulation, Mathy et al. [55] pointed out that the permeability of coal would greatly affect the cavity growth process, and the growth direction was towards the high permeability region. Nourozieh et al. [50] indicated that the rock interlayer would limit the cavity growth process in the vertical direction in the coal seam.

The moisture content in the coal seam acts on the cavity growth process by affecting the coal gasification reaction and the temperature field. Pang et al. [56] and Verma et al. [57] declared that when the moisture content was small, the moisture was conducive to increasing the H<sub>2</sub> content in the syngas, raising the temperature in the cavity, and growing the cavity. In contrast, when the moisture content was large, the phase transformation and decomposition of water would consume a lot of heat energy, thus reducing the gasification efficiency and hindering cavity growth. Shirazi et al. [51] established a cavity growth model under coal moisture content of 5%, 10%, and 20%. The results showed that when the moisture content was 5%, the growth rate of the cavity volume was obviously higher than that of the other two groups.

###### 4.1.2. Types of Coal

Although there is no consistent view on the relationship between coal rank and permeability, most studies point out that the higher the coal rank is, the lower the permeability of coal is. Perkins and Sahajwalla [42] concluded that low-rank coal was conducive to the cavity growth by numerical simulation. Liu et al. [58] and Li et al. [59] agreed that lignite was suitable for cavity growth due to its well-developed pores and high reactivity, while gas coal, fat coal, and lean coal were prone to producing cinder accumulation after gasification, which was not conducive to cavity growth. Moreover, the heterogeneity of the coal structure and coal physical properties would also affect the geometry and growth rate of the cavity.

##### 4.2. Operating Factors

The operating factors mainly include the temperature, the pressure, the composition of the gasification agent, and the flow pattern of the gasification agent.

#### 4.2.1. The Temperature

During the UCG process, the temperature distribution of different regions in the cavity is not uniform, with the range of 600–1500 °C [3,11,17,60]. When the temperature is low, the gasification reaction is less efficient or even impossible. On the contrary, when the temperature is high, the coal ash will melt and adhere to the coal wall, affecting the subsequent gasification process [11,61]. By numerical model, Massaquoi and Riggs [38,39] demonstrated that reducing ash region thickness could improve oxygen flux and lead to a higher combustion rate, which accelerated cavity growth. Furthermore, the temperature also significantly directly affects the physical properties of coal. For example, coal's permeability, porosity, specific heat capacity, and thermal conductivity increased obviously when the temperature exceeded 300 °C [60,62]. Shirazi et al. [51] demonstrated that the increase in thermal conductivity of coal would promote cavity growth.

#### 4.2.2. The Pressure

In order to control the gas flow, the pressure in the UCG cavity is often balanced with the hydrostatic pressure of the gasification coal seam. Usually, the pressure in the cavity depends on the depth of the coal seam, increasing at a rate of 1 MPa/100 m.

The pressure has a positive effect on various gasification reactions. It accelerates the coal consumption of the cavity sidewall, thereby promoting the cavity growth [3,63]. Kariznovi et al. [64–66] illustrated that the reaction rate increases with the pressure. However, when the pressure further increases to a certain extent, the effect of pressure on the reaction rate decreases. Shirazi et al. [67] believed that the reaction rate of the main reactions in UCG depended on the partial pressure of oxygen. Shirazi demonstrated that increasing the pressure from 0.1 MPa to 1 MPa would enhance the cavity growth rate by numerical simulation. Meanwhile, Jowkar et al. [68] also argued that increasing pressure appears to be economically beneficial in UCG.

Notably, at present, most of the coal gasification experiments are conducted under low-pressure conditions. Due to instrument limitations, the kinetic data of coal gasification reaction under high-pressure conditions (>5 MPa) cannot be directly measured. In the current numerical model, the kinetic parameters are mostly obtained by combining field test data and suitable algorithms (such as the Levenberg–Marquardt algorithm) [50].

#### 4.2.3. The Composition of Gasification Agent

Common gasification agents are air, oxygen-enriched, air–water vapor, and air–carbon dioxide. The effective reactive species in the gasification agent are oxygen, water vapor, and carbon dioxide. In general, oxygen determines the base rate of cavity growth. An appropriate amount of water vapor can further increase the cavity growth rate. While CO<sub>2</sub> can slow down the cavity growth, making it grow more balanced in all directions.

Javed et al. [69] compared the cavity volume variation with time under different oxygen concentrations (15%, 20%, and 25%) and different types of gasification agents (air–steam and air) through the 3D-CFD numerical model. The results showed that the cavity volume increases with the oxygen concentration at the same time. Moreover, the cavity volume growth rate corresponding to the air–steam agent is slightly higher than that corresponding to air agent in the initial period and obviously higher in a long period.

#### 4.2.4. Flow Pattern of Gasification Agent

The flow pattern of gasification agent contains flow velocity and flow direction. Via experiments and numerical models, Daggupati et al. [30,31,70] and Prabu et al. [32,71] expressed that the gasification agent's flow pattern greatly influences the cavity's shape, making it grow at different rates in all directions.

For the LVW-UCG technique, the gasification agent flows vertically and rapidly from the gas injection well, then reaches the coal seam bottom and bounces around. After that, the airflow forms an oblate spheroid and eventually flows out along the gasification channel. During this process, the gasification agent continuously reacts with coal. Therefore, the

shape of the cavity was similar to a teardrop, with the head facing the gas injection end and the tail facing the gas production end.

For the CRIP-UCG technique, the flow rate of the gasification agent is high at the gas injection inlet end, meaning that the combustibles on the wall of the channel cannot fully react with the gasification agent. So, the cross-sectional of the channel at the inlet end is small and symmetrical. When the void space is formed on the horizontal channel, the flow rate of the gasification agent gradually slows down due to the increase in volume. At this period, the gas flow first contacts the cavity side wall closer to the outlet. Then, it returns to the gas injection end along the side wall, forming a vortex. The gasification agent concentration at the beginning of the vortex is high, which can consume more coal mass. During the continuous reciprocating process, the cavity gradually becomes teardrop-shaped, with the head facing the gas production end and the tail facing the gas injection end. Figure 13 shows the flow field distribution of gasification agent in different cavities. It can be seen that at a specific injection flow rate, the flow field distribution of the gasification agent is fuller in the cavity with the right teardrop shape.

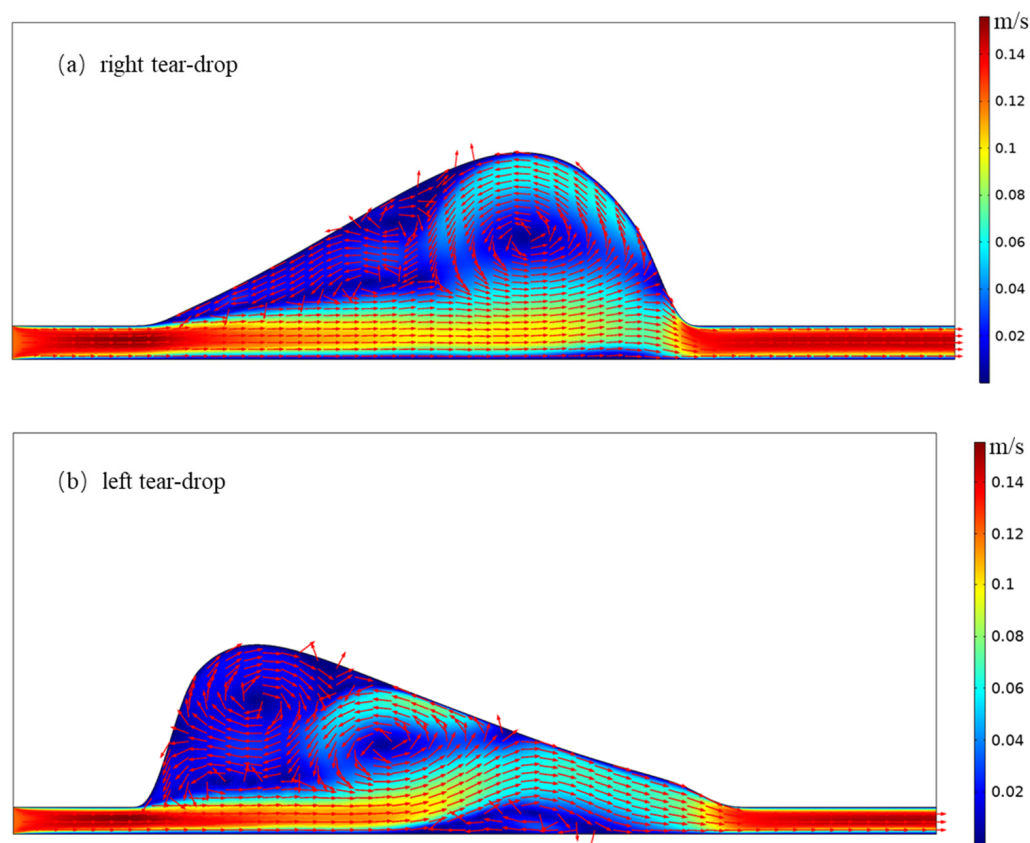


**Figure 13.** Flow field distribution in cavity with right/left teardrop shape.

#### 4.3. Chapter Summary

The cavity growth process is mainly controlled by geological factors and operating factors.

Geological factors are mainly coal seam physical properties and coal types. The coal seam's physical properties include permeability and moisture content. The permeability determines the flow path of the gasification agent and directly affects the shape of the cavity. The higher the permeability, the faster the cavity growth. The moisture content in the coal seam acts on the cavity growth process by affecting the coal gasification reaction and the temperature field. Proper moisture is beneficial for cavity growth. For coal types, low-rank coal is more suitable for UCG.

The operating factors mainly include the temperature, the pressure, the composition of gasification agent, and flow pattern of gasification agent. The temperature distribution

in the cavity is complex. When the temperature is low, the gasification reaction is less efficient or even impossible. When the temperature is high, the coal ash will melt and adhere to the coal wall, affecting the subsequent gasification process. The pressure of the cavity is proportional to the depth of the coal seam, and the cavity growth rate increases with the pressure. For several types of gasification agents, oxygen determines the base rate of cavity growth. Proper water can further increase the cavity growth rate, while CO<sub>2</sub> can slow down the cavity growth. The flow pattern of the gasification agent greatly influences the cavity's shape, where the cavity growth rate is higher in the region with high gasification-agent concentration.

## 5. Existing Problems and Research Trends

### 5.1. Existing Problems

UCG is a comprehensive system of interdisciplinary engineering research, which not only involves the coupling theory of multiple physical–chemical fields, but also covers the application of engineering technology. Table 2 shows buried-depth statistics of UCG field tests. As shown in Table 2, a mature technical system has been formed for UCG in shallow coal seams. However, the functional design of UCG in deep coal seams is still in the exploratory stage. From Figure 14, the reaction product tendency is different at different depths of coal seam, which is related to steam gasification, water gas shift, inversed CO methanation, and other reactions. Moreover, a deep UCG features a longer residence time for dehydration and gasification of coal, and a shorter residence time for coal pyrolysis and combustion [54]. The difference of reactions in different depth environment conditions will affect the cavity growth. In order to promote the implementation of a UCG project in deep coal seams, the following problems need to be solved urgently:

- (1) Cavity growth is the result of the complex interaction of numerous physical and chemical fields. LVW-UCG is suitable for shallow coal seams, while CRIP-UCG is suitable for deep coal seams. The gasification agent flow patterns corresponding to the LVW and CRIP types are obviously different. Moreover, the thermophysical conditions of UCG in the deep coal seam have changed hugely. However, the current research results of UCG are mostly based on LVW type in shallow coal seam, which cannot effectively guide the production of a CRIP-UCG project in a deep coal seam.
- (2) The variation in moisture content and its distribution in the coal seam will act on heat balance and material balance in the cavity through a series of physical and chemical processes. This will make the movement and rupture behavior of the cavity side wall unknown in the process of gasification deformation, which seriously affects the quality of the UCG project. However, at present, the research results of the UCG cavity growth behavior under the condition of a water-bearing coal seam are few in number and mainly qualitative descriptions lacking quantitative analysis.

**Table 2.** Buried-depth statistics of UCG field tests (modified from [3,9,16]).

Country	Test Site	Year	Seam Depth (m)	Technique
U.S.S.R	Podmoskova	1940–1962	40	LVW
	Shatskaya	1959	50	LVW
	Angrenskaja	1961	150	LVW
USA	Hanna series tests	1973–1977	85–120	LVW
	Hoe Creek series tests	1976–1979	40	LVW
	Rawlins series tests	1979	105–180	
	Pricetown	1979	270	LVW
	Centralia series tests	1984–1985	75	LVW/CRIP
	Rocky Mountain	1987–1988	110	LVW/CRIP

Table 2. Cont.

Country	Test Site	Year	Seam Depth (m)	Technique
France	Bruayen Artois	1979–1981	1170	Drilling-type
	Haute-Duele	1985–1986	880	
Belgium	Thulin	1982–1984	860	LVW
Spain	El Tremedal	1997	500–700	CRIP
Australia	Chinchilla series tests	2000–2013	130	CRIP
	Bloodwood Ck series tests	2009–2011	200	
South Africa	Majuba test	2007–2011	250–380	Drilling-type
Poland	Wieczorek	2014	464	
China	Xinwen, Xuzhou, Tangshan, Gansu	1985–2010	80–200	Shaft type
	Ulanqab	2007–2012	285	
Canada	Swan Hills	2007–2012	1400	CRIP

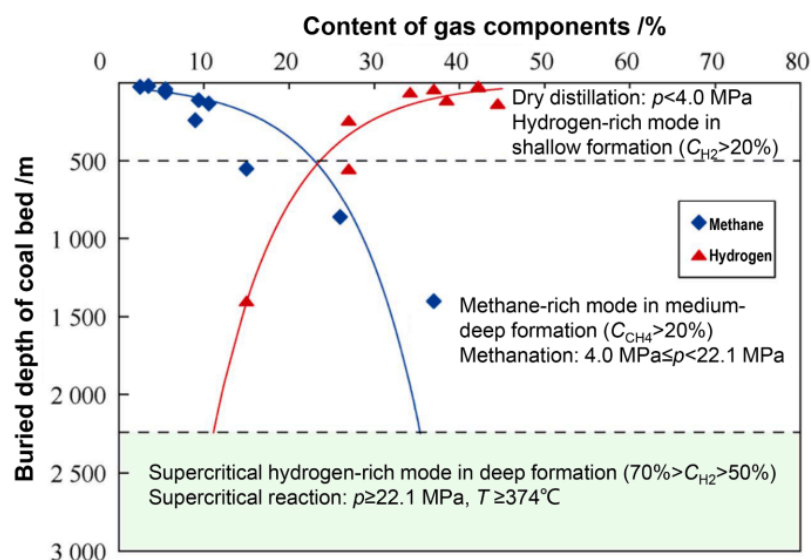


Figure 14. Three exploitation modes of UCG (from [3]).

### 5.2. Research Trends

At present, the development of UCG technology is at a new stage of innovation and breakthrough, and the main research focus has shifted from field tests to two new focuses:

- (1) Laboratory experimental research under conditions similar to actual coal seams. Study the cavity growth mechanism of CRIP-type in the deep coal seam. Focus on conducting large-scale coal gasification experimental research under high-pressure conditions. Furthermore, reveal the gasification mechanism of different operation regions (cavity sidewall, void space, and deposit), the cavity growth behaviors, and the influence of fractures on fluid flow. Meanwhile, improve the measurement method of the parameters required by the numerical model. Emphatically, study the influence mechanism of moisture content and its distribution in a coal seam on cavity growth. Elucidate the variation characteristics of heat and mass transfer in the cavity under the condition of water-bearing/non-water-bearing coal seams, determining the moisture content that can maintain the effective operation of the UCG reaction, clarifying the proper moisture content that can increase the hydrogen content in the syngas, and illustrating the effect of moisture content on the movement mechanism of the cavity side wall.

- (2) Numerical simulation research considering chemical reaction, thermal field propagation, complex fluid flow, coal rock deformation, and seepage field. It is meaningful to refine a single physical field model based on experimental results to obtain a more accurate expression. Moreover, one should establish a multi-field coupling numerical model of the CRIP-UCG, clarifying the heat and mass transfer characteristics of the cavity during the gasification process, as well as the movement mechanism of the cavity side wall. In order to improve the stability and convergence of the multi-field model, an advanced coupling algorithm is needed to solve the thermal–fluid flow–chemical–mechanical coupling problem. Moreover, utilizing machine learning to predict UCG data (such as syngas concentration, syngas calorific value, and underground temperature) is also promising for UCG projects.

**Author Contributions:** Project administration, H.F.; Conceptualization, Y.L.; Supervision, T.G.; Writing–original draft preparation, T.Z.; Investigation, Y.Y.; Writing–Review & Editing, D.L., J.D. and L.L. All authors have read and agreed to the published version of the manuscript.

**Funding:** This work was supported by the Major special projects of CNPC science and technology (2019E025).

**Institutional Review Board Statement:** Not applicable.

**Informed Consent Statement:** Not applicable.

**Data Availability Statement:** Not applicable.

**Acknowledgments:** We appreciate the support by the Major special projects of CNPC science and technology (2019E025).

**Conflicts of Interest:** The authors declare no conflict of interest.

## References

1. Caineng, Z.O.U.; Xiong, B.; Huaqing, X.U.E.; Zheng, D.; Zhixin, G.E.; Ying, W.A.N.G.; Jiang, L.; Songqi, P.A.N.; Songtao, W.U. The role of new energy in carbon neutral. *Pet. Explor. Dev.* **2021**, *48*, 480–491.
2. Ludwik-Pardała, M.; Stańczyk, K. Underground coal gasification (UCG): An analysis of gas diffusion and sorption phenomena. *Fuel* **2015**, *150*, 48–54. [[CrossRef](#)]
3. Caineng, Z.O.U.; Yanpeng, C.H.E.N.; Lingfeng, K.O.N.G.; Fenjin, S.; Shanshan, C.; Zhen, D. Underground coal gasification and its strategic significance to the development of natural gas industry in China. *Pet. Explor. Dev.* **2019**, *46*, 205–215.
4. Lingfeng, K.; Zhongxun, Z.; Binggang, Z. Feasibility analysis on rebuilding coal-mine gas storage by using underground coal gasification (UCG) technology. *Nat. Gas Ind.* **2016**, *36*, 99–107. (In Chinese)
5. Yang, D.; Koukouzas, N.; Green, M.; Sheng, Y. Recent development on underground coal gasification and subsequent CO<sub>2</sub> storage. *J. Energy Inst.* **2016**, *89*, 469–484. [[CrossRef](#)]
6. Najafi, M.; Jalali, S.M.E.; KhaloKakaie, R.; Forouhandeh, F. Prediction of cavity growth rate during underground coal gasification using multiple regression analysis. *Int. J. Coal Sci. Technol.* **2015**, *2*, 318–324. [[CrossRef](#)]
7. Yuewu, L.; Huijun, F.; Longlong, L.; Tengze, G.; Taiyi, Z.; Danlu, L.; Jiuge, D. Recent progress on numerical research of key mechanical problems during underground coal gasification. *Chin. J. Theor. Appl. Mech.* **2022**, *54*, 1–17. (In Chinese)
8. Klimenko, A.Y. Early developments and inventions in underground coal gasification. In *Underground Coal Gasification and Combustion*; Woodhead Publishing: Sawston, UK, 2018; pp. 11–24.
9. Perkins, G. Underground coal gasification—Part I: Field demonstrations and process performance. *Prog. Energy Combust. Sci.* **2018**, *67*, 158–187. [[CrossRef](#)]
10. Perkins, G. Mathematical modelling of in situ combustion and gasification. *Proc. Inst. Mech. Eng. Part A J. Power Energy* **2018**, *232*, 56–73. [[CrossRef](#)]
11. Perkins, G. Underground coal gasification—Part II: Fundamental phenomena and modeling—ScienceDirect. *Prog. Energy Combust. Sci.* **2018**, *67*, 234–274. [[CrossRef](#)]
12. Perkins, G.; du Toit, E.; Cochrane, G.; Bollaert, G. Overview of underground coal gasification operations at Chinchilla, Australia. *Energy Sources Part A Recovery Util. Environ. Eff.* **2016**, *38*, 3639–3646. [[CrossRef](#)]
13. Upadhye, R.S.; Field, J.E.; Fields, D.B.; Britten, J.A.; Thorsness, C.B. *Experimental Investigation of Coal Spalling*; Lawrence Livermore National Lab.: Livermore, CA, USA, 1986.
14. Gao, W.; Zagorščak, R.; Thomas, H.R. Insights into solid-gas conversion and cavity growth during Underground Coal Gasification (UCG) through Thermo-Hydraulic-Chemical (THC) modelling. *Int. J. Coal Geol.* **2021**, *237*, 103711. [[CrossRef](#)]
15. Laouafa, F.; Farret, R.; Vidal-Gilbert, S.; Kazmierczak, J.B. Overview and modeling of mechanical and thermomechanical impact of underground coal gasification exploitation. *Mitig. Adapt. Strateg. Glob. Change* **2016**, *21*, 547–576. [[CrossRef](#)]

16. Bhutto, A.W.; Bazmi, A.A.; Zahedi, G. Underground coal gasification: From fundamentals to applications. *Prog. Energy Combust. Sci.* **2013**, *39*, 189–214. [CrossRef]
17. Bhaskaran, S.; Samdani, G.; Aghalayam, P.; Ganesh, A.; Singh, R.P.; Sapru, R.K.; Jain, P.K.; Mahajani, S. Experimental studies on spalling characteristics of Indian lignite coal in context of underground coal gasification. *Fuel* **2015**, *154*, 326–337. [CrossRef]
18. Niu, S.; Zhao, Y.; Hu, Y. Experimental investigation of the temperature and pore pressure effect on permeability of lignite under the in situ condition. *Transp. Porous Media* **2014**, *101*, 137–148. [CrossRef]
19. Stephens, D.R. *Hoe Creek Experiments: LLNL's Underground Coal-Gasification Project in Wyoming*; Lawrence Livermore National Lab.: Livermore, CA, USA, 1981.
20. Hill, R.W.; Thorsness, C.B. Large block experiments in underground coal gasification. *ACS Symp. Ser.* **1983**, *79*, 226.
21. Blinderman, M.S.; Klimenko, A.Y. *Underground Coal Gasification and Combustion*; Woodhead Publishing: Sawston, UK, 2017.
22. Thorsness, C.B. 3.4 an underground coal gasification cavity simulator with solid motion. *Fossil Energy* **1983**. Available online: [https://digital.library.unt.edu/ark:/67531/metadc1065489/m2/1/high\\_res\\_d/5295596.pdf](https://digital.library.unt.edu/ark:/67531/metadc1065489/m2/1/high_res_d/5295596.pdf) (accessed on 1 November 2022).
23. Cena, R.J.; Britten, J.A.; Thorsness, C.B. *Excavation of the Partial Seam CRIP Underground Coal Gasification Test Site*; Lawrence Livermore National Lab.: Livermore, CA, USA, 1987.
24. Stephens, D.R.; Cena, R.J.; Hill, R.W.; Thorsness, C.B. The Centralia partial seam CRIP underground coal gasification experiment. [Controlled retracting injection point]. In Proceedings of the AIChE Annual Meeting, San Francisco, CA, USA, 25 November 1984; American Institute of Chemical Engineers: New York, NY, USA, 1985.
25. Cena, R.J.; Hill, R.W.; Stephens, D.R.; Thorsness, C.B. *Summary Results of the Centralia Partial Seam CRIP Underground Coal Gasification Field Test*; Lawrence Livermore National Lab.: Livermore, CA, USA, 1984.
26. Kühnel, R.A.; Schmit, C.R.; Eylands, K.E.; McCarthy, G.J. Comparison of the pyrometamorphism of clayey rocks during underground coal gasification and firing of structural ceramics. *Appl. Clay Sci.* **1993**, *8*, 129–146. [CrossRef]
27. Oliver, R.L.; Lindblom, S.R.; Covell, J.R. *Results of Phase 2 Postburn Drilling, Coring, and Logging: Rocky Mountain 1 Underground Coal Gasification Test, Hanna, Wyoming*; Western Research Institute: Laramie, WY, USA, 1991.
28. Cena, R.J.; Thorsness, C.B.; Britten, J.A. *Assessment of the CRIP (Controlled Retracting Injection Point) Process for Underground Coal Gasification: The Rocky Mountain I Test*; Lawrence Livermore National Lab.: Livermore, CA, USA, 1988.
29. Kapusta, K.; Stańczyk, K.; Wiatowski, M.; Češko, J. Environmental aspects of a field-scale underground coal gasification trial in a shallow coal seam at the Experimental Mine Barbara in Poland. *Fuel* **2013**, *113*, 196–208. [CrossRef]
30. Daggupati, S.; Mandapati, R.N.; Mahajani, S.M.; Ganesh, A.; Mathur, D.K.; Sharma, R.K.; Aghalayam, P. Laboratory studies on combustion cavity growth in lignite coal blocks in the context of underground coal gasification. *Energy* **2010**, *35*, 2374–2386. [CrossRef]
31. Daggupati, S.; Mandapati, R.N.; Mahajani, S.M.; Ganesh, A.; Sapru, R.K.; Sharma, R.K.; Aghalayam, P. Laboratory studies on cavity growth and product gas composition in the context of underground coal gasification. *Energy* **2011**, *36*, 1776–1784. [CrossRef]
32. Prabu, V.; Jayanti, S. Simulation of cavity formation in underground coal gasification using bore hole combustion experiments. *Energy* **2011**, *36*, 5854–5864. [CrossRef]
33. Kapusta, K.; Stańczyk, K. Pollution of water during underground coal gasification of hard coal and lignite. *Fuel* **2011**, *90*, 1927–1934. [CrossRef]
34. Kapusta, K.; Wiatowski, M.; Stańczyk, K. An experimental ex-situ study of the suitability of a high moisture ortho-lignite for underground coal gasification (UCG) process. *Fuel* **2016**, *179*, 150–155. [CrossRef]
35. Wang, Z.; Wei, Y.; Hou, T.; Jin, Y.; Wang, C.; Liang, J. Large-scale laboratory study on the evolution law of temperature fields in the context of underground coal gasification. *Chin. J. Chem. Eng.* **2020**, *28*, 3126–3135. [CrossRef]
36. Winslow, A.M. Numerical model of coal gasification in a packed bed. In *Symposium (International) on Combustion*; Elsevier: Amsterdam, The Netherlands, 1977; Volume 16, pp. 503–513.
37. Tsang, T.H.T. *Modeling of Heat and Mass Transfer during Coal Block Gasification*; The University of Texas at Austin: Austin, TX, USA, 1980.
38. Massaquoi JG, M.; Riggs, J.B. Mathematical modeling of combustion and gasification of a wet coal slab—I: Model development and verification. *Chem. Eng. Sci.* **1983**, *38*, 1747–1756. [CrossRef]
39. Massaquoi JG, M.; Riggs, J.B. Mathematical modeling of combustion and gasification of a wet coal slab—II: Mode of combustion, steady state multiplicities and extinction. *Chem. Eng. Sci.* **1983**, *38*, 1757–1766. [CrossRef]
40. Park, K.Y.; Edgar, T.F. Modeling of early cavity growth for underground coal gasification. *Ind. Eng. Chem. Res.* **1987**, *26*, 237–246. [CrossRef]
41. Perkins, G.; Sahajwalla, V. A mathematical model for the chemical reaction of a semi-infinite block of coal in underground coal gasification. *Energy Fuels* **2005**, *19*, 1679–1692. [CrossRef]
42. Perkins, G.; Sahajwalla, V. A numerical study of the effects of operating conditions and coal properties on cavity growth in underground coal gasification. *Energy Fuels* **2006**, *20*, 596–608. [CrossRef]
43. Perkins, G.; Sahajwalla, V. Steady-state model for estimating gas production from underground coal gasification. *Energy Fuels* **2008**, *22*, 3902–3914. [CrossRef]
44. Luo, Y.; Coertzen, M.; Dumble, S. Comparison of UCG cavity growth with CFD model predictions. In Proceedings of the Seventh International Conference on CFD in the Minerals and Process Industries (CSIRO), Melbourne, Australia, 9–11 December 2009.
45. Samdani, G.; Aghalayam, P.; Ganesh, A.; Sapru, R.K.; Lohar, B.L.; Mahajani, S. A process model for underground coal gasification—Part-I: Cavity growth. *Fuel* **2016**, *181*, 690–703. [CrossRef]

46. Samdani, G.; Aghalayam, P.; Ganesh, A.; Sapru, R.K.; Lohar, B.L.; Mahajani, S. A process model for underground coal gasification–Part-II growth of outflow channel. *Fuel* **2016**, *181*, 587–599. [[CrossRef](#)]
47. Samdani, G.; Aghalayam, P.; Ganesh, A.; Mahajani, S. A process model for underground coal gasification–Part-III: Parametric studies and UCG process performance. *Fuel* **2018**, *234*, 392–405. [[CrossRef](#)]
48. Xin, L.; Wang, Z.; Huang, W.; Kang, G.; Lu, X.; Zhang, P.; Wang, J. Temperature field distribution of burnt surrounding rock in UCG stope. *Int. J. Min. Sci. Technol.* **2014**, *24*, 573–580. [[CrossRef](#)]
49. Jowkar, A.; Sereshki, F.; Najafi, M. A new model for evaluation of cavity shape and volume during Underground Coal Gasification process. *Energy* **2018**, *148*, 756–765. [[CrossRef](#)]
50. Nourozieh, H.; Kariznovi, M.; Chen, Z.; Abedi, J. Simulation study of underground coal gasification in Alberta reservoirs: Geological structure and process modeling. *Energy Fuels* **2010**, *24*, 3540–3550. [[CrossRef](#)]
51. Sarraf Shirazi, A.; Karimipour, S.; Gupta, R. Numerical simulation and evaluation of cavity growth in in situ coal gasification. *Ind. Eng. Chem. Res.* **2013**, *52*, 11712–11722. [[CrossRef](#)]
52. Seifi, M.; Chen, Z.; Abedi, J. Numerical simulation of underground coal gasification using the CRIP method. *Can. J. Chem. Eng.* **2011**, *89*, 1528–1535. [[CrossRef](#)]
53. Kasani, H.A.; Chalaturnyk, R.J. Coupled reservoir and geomechanical simulation for a deep underground coal gasification project. *J. Nat. Gas Sci. Eng.* **2017**, *37*, 487–501. [[CrossRef](#)]
54. Jiang, L.; Chen, S.; Chen, Y.; Chen, Z.; Sun, F.; Dong, X.; Wu, K. Underground coal gasification modelling in deep coal seams and its implications to carbon storage in a climate-conscious world. *Fuel* **2023**, *332*, 126016. [[CrossRef](#)]
55. Mathy, B. Flow modeling in an underground gasifier at great depth by the boundary element method. *Fuel Energy Abstr.* **1995**, *4*, 254.
56. Pang, X.L.; Chen, F. Model test research on the temperature field of underground coal gasification with water influx and oxygen-enriched. *J. China Coal Soc.* **2011**, *36*, 151–155. (In Chinese)
57. Verma, R.P.; Mandal, R.; Chaulya, S.K.; Singh, P.K.; Singh, A.K.; Prasad, G.M. Contamination of groundwater due to underground coal gasification. *Int. J. Water Resour. Environ. Eng.* **2014**, *6*, 303–311.
58. Liu, S.; Liang, J.; Yu, X.; Lu, L. Characteristics of underground gasification of different kinds of coal. *J. China Univ. Min. Technol.* **2003**, *32*, 624–628. (In Chinese)
59. Li, H.; Guo, G.; Zheng, N. Influence of coal types on overlying strata movement and deformation in underground coal gasification without shaft and prediction method of surface subsidence. *Process Saf. Environ. Prot.* **2018**, *120*, 302–312. [[CrossRef](#)]
60. Liu, X.; Guo, G.; Li, H. Study on the propagation law of temperature field in surrounding rock of underground coal gasification (UCG) combustion cavity based on dynamic thermal parameters. *Results Phys.* **2019**, *12*, 1956–1963. [[CrossRef](#)]
61. Liu, S.Q.; Wang, Y.Y.; Ke, Z.; Ning, Y.A.N.G. Enhanced-hydrogen gas production through underground gasification of lignite. *Min. Sci. Technol.* **2009**, *19*, 389–394. [[CrossRef](#)]
62. Jiang, L.; Chen, Z.; Ali SM, F. Thermal-hydro-chemical-mechanical alteration of coal pores in underground coal gasification. *Fuel* **2020**, *262*, 116543. [[CrossRef](#)]
63. Wall, T.F.; Liu, G.S.; Wu, H.W.; Roberts, D.G.; Benfell, K.E.; Gupta, S.; Lucas, J.A.; Harris, D.J. The effects of pressure on coal reactions during pulverised coal combustion and gasification. *Prog. Energy Combust. Sci.* **2002**, *28*, 405–433. [[CrossRef](#)]
64. Kariznovi, M.; Nourozieh, H.; Abedi, J.; Chen, Z. Simulation study and kinetic parameter estimation of underground coal gasification in Alberta reservoirs. *Chem. Eng. Res. Des.* **2013**, *91*, 464–476. [[CrossRef](#)]
65. MacNeil, S.; Basu, P. Effect of pressure on char combustion in a pressurized circulating fluidized bed boiler. *Fuel* **1998**, *77*, 269–275. [[CrossRef](#)]
66. Makino, M.; Toda, Y. Factors affecting methane evolution on pyrolysis of coal under pressure. *Fuel* **1979**, *58*, 231–234. [[CrossRef](#)]
67. Shirazi, A.S. CFD Simulation of Underground Coal Gasification. In *Masters Abstracts International*; University Microfilms International: Edmonton, AB, Canada, 2012; Volume 51.
68. Jowkar, A.; Sereshki, F.; Najafi, M. Numerical simulation of UCG process with the aim of increasing calorific value of syngas. *Int. J. Coal Sci. Technol.* **2020**, *7*, 196–207. [[CrossRef](#)]
69. Javed, S.B.; Uppal, A.A.; Bhatti, A.I.; Samar, R. Prediction and parametric analysis of cavity growth for the underground coal gasification project Thar. *Energy* **2019**, *172*, 1277–1290. [[CrossRef](#)]
70. Daggupati, S.; Mandapati, R.N.; Mahajani, S.M.; Ganesh, A.; Pal, A.K.; Sharma, R.K.; Aghalayam, P. Compartment modeling for flow characterization of underground coal gasification cavity. *Ind. Eng. Chem. Res.* **2011**, *50*, 277–290. [[CrossRef](#)]
71. Prabu, V.; Jayanti, S. Laboratory scale studies on simulated underground coal gasification of high ash coals for carbon-neutral power generation. *Energy* **2012**, *46*, 351–358. [[CrossRef](#)]